

Analysis of Dexterity Motion by Singular Value Decomposition for Hand Movement Measured Using Inertial Sensors

Keisuke Kitano, Akihito Ito, and Nobutaka Tsujiuchi, *Member, IEEE-EMBS*

Abstract— Finger movements play an important role in many daily human actions. Among the studies on the dexterity of fingers required for various tasks in neurology and simple evaluation tests, few have focused on detailed finger movements themselves. Therefore, in this study, we improved the hand motion measurement system using inertial sensors and the motion analysis method developed in our previous study and measured the motion of the upper limbs (including the fingers) during a general finger dexterity test. By applying singular value decomposition to the obtained joint angles and decomposing them into simpler movement units, we obtained the timing of each movement unit and the purpose of each movement as the coordination state of the joints. By applying hierarchical clustering to multiple trials in a finger dexterity test, we also determined the similarity between trials and investigated the characteristics of movements with higher dexterity. We investigated the motor characteristics in finger dexterity by analyzing our results.

I. INTRODUCTION

In recent years, demand has been increasing for the development of daily life support devices and workload-free environments based on human movement characteristics against the extension of healthy life expectancy and physical rehabilitation in super-aging societies and improving the efficiency of industrial activities. To meet these requirements, every kind of human movement must be evaluated for which appropriate measurements and analysis are required. In particular, hand movements must be analyzed because they are essential for a variety of life and work. These hand motions, which are collectively referred to as finger dexterity, invariably decline with age and are related to cognitive functions [1]. Therefore, understanding hand and finger dexterity in activities and assessing their movements are important to identify clumsy motions and to improve dexterity.

Such research on dexterity has mainly been conducted in the neurotransmission and clinical fields [2], [3]. In addition, a pegboard, which is a common evaluation method for finger dexterity, is based only on the achievement time of a given movement [4], and insufficient examples focus on the motion state during dexterity movements. Although hand movements have previously been evaluated, most studies failed to scrutinize them as closely as the lower limbs or gaits. Instead, they were performed under such conditions as simplified models, movement restrictions, and only using the changes in external devices.

Therefore, we focus on hand dexterity and meticulously measure the upper limb and finger movements with the inertial

sensor systems. Then from accurately acquired 3D joint angle changes, we studied the kinematic characteristics of dexterity by focusing on the coordination relationship of joints and timing. We used singular value decomposition (SVD) and clustering to analyze and visualize the characteristics as time transition and the coordination relationship of the joint angles related to the hand movements.

II. METHODS

A. Measurement System and Sensor Postures

We measure the upper limb movements included in the hand and fingers with hand-motion measurement system, and IMS-SD (Tec Gihan Co., Ltd., Japan). The former hand system has a total of 20, MEMS-type 9-axis inertial sensors with a compass (MPU9250, InvenSens), hereafter called the Inertial Measurement Unit (IMU). IMS-SD is a commercial wireless (Bluetooth) IMU system that outputs the identical kind values as the above system. By attaching both systems to the human upper limbs and measuring synchronously, we can measure the dexterity hand movements and their associated upper body parts (Fig. 1).

The IMU postures (from the IMU to global coordinate systems) are estimated from their outputs, and the global coordinate system is defined so that the z-axis is vertical upward related to the direction of the gravitational acceleration, and the x-axis is the azimuth direction. In this study, we calculated the initial posture as Euler angles, and converted them to the quaternion, which was updated during movements by angular velocity. Since the integration error of angular velocity is often a problem in posture updates, in our previous study we corrected it using the constructed observation equations of an extended Kalman filter [5]. However, since that state and the observation equations are for Euler angles, we adapted them to quaternion by changing Euler to quaternion in the state equation and adding a constraint equation where the norm of the quaternion is 1 in the observation equation.

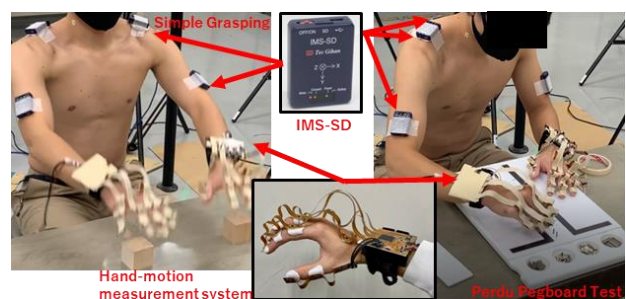


Figure 1. IMU measurement systems and attachment positions

Keisuke Kitano is with the Organization for Research Initiatives and Development, and Faculty of Science and Engineering, Doshisha University, Kyotanabe, Kyoto 610-0321 Japan (e-mail: kkitano@mail.doshisha.ac.jp).

Akihito Ito and Nobutaka Tsujiuchi are with the Mechanical Engineering Department, Doshisha University, Kyotanabe, Kyoto 610-0321 Japan (e-mail: aito@mail.doshisha.ac.jp, ntsujiuc@mail.doshisha.ac.jp).

B. Hand and Upper Limb Link Models

In our previous study, we proposed a method that estimates the body link length and made hand and finger models [5]. In this method, the position vectors from the target joint center to IMUs are estimated by combining the IMU outputs in the rotational motions of two joint axes in that joint and making a link model based on multiple position vectors and the relative relationships among IMUs. In this paper, the collarbone, the upper arm, the forearm, the hand, and each phalanx are assumed to be rigid bodies (segments), and one IMU of the measurement system is attached to each segment. Therefore, the fingertip position (the edge of the n^{th} segment) in the global coordinate system (${}^G\mathbf{P}_n$) is calculated by regarding the sternoclavicular joint as the origin:

$${}^G\mathbf{P}_n = \sum_{i=1}^n \mathbf{R}(\mathbf{q}_i)^i \mathbf{p}_i, \quad (1)$$

where $\mathbf{R}(\mathbf{q}_i)$ is a rotational matrix by the IMU quaternion posture on the i^{th} segment, and \mathbf{p}_i is the i^{th} segment vector in the i^{th} IMU coordinate system. The joint axes are identified from the joint rotation data during the above estimation and combined with the link vectors of each segment to define the coordinate system of each segment. The joint angle is defined as the relative postures (Euler angles) between the coordinate systems of the two segments adjacent to the target joint.

C. Singular Value Decomposition and Clustering

To analyze and evaluate finger dexterity, a movement is decomposed using SVD for the measured parameters (joint angles in this case). Because human dexterity movements are composed of more simple movement units, the movement units can be extracted (each decomposed mode) to understand the coordination relationship of the joints and the timing in each unit. We defined the joint angle matrix to which the SVD is applied as matrix \mathbf{A} such that the row direction indicates the time variation and the column direction indicates each joint axis of each joint. Therefore, we obtained a decomposed result:

$$\mathbf{A} - \mathbf{A}_{\text{ave}} = \mathbf{U}\mathbf{A}\mathbf{V}^T = \sum_{m=1}^N s_m \mathbf{u}_m \mathbf{v}_m^T, \quad (2)$$

where \mathbf{A}_{ave} is the time average of \mathbf{A} , left singular value vector \mathbf{u} is the time history change that can be regarded as the timing, and right singular value vector \mathbf{v} is the joint coordination and joint contribution. The diagonal component s_m indicates the contribution of m^{th} mode. N is the number of degrees of freedom of the joint and the number of columns of \mathbf{A} .

In addition, the decomposed results are expected to show differences among individuals and even among the same subject in identical types of movements. Therefore, we use agglomerative hierarchical clusters to classify the decomposed results in each mode to understand similar movement units. In agglomerative hierarchical clustering, several methods have calculated the distance between two clusters. In this study, we used Ward's linkage method, which is an internal square distance used for classification in a previous research on walking [6]. Distance d between cluster l and r is calculated:

$$d(l, r) = \sqrt{(2n_l n_r) / (n_l + n_r)} \|\bar{\mathbf{x}}_l - \bar{\mathbf{x}}_r\|_2, \quad (3)$$

where $\|\cdot\|_2$ is the Euclidean distance, $\bar{\mathbf{x}}_l$ and $\bar{\mathbf{x}}_r$ are the centroids for \mathbf{u} or \mathbf{v} , and n_l and n_r are the number of elements of clusters l and r . We apply this method to the left and right singular value vectors, which are the above SVD results. Since the left singular value vector is time-series data, we treat the data of each time step as an observation value to understand the similarity of each trial and each mode. Since the movement times are different, the time step is resampled to make the identical lengths when clustering is applied.

III. MEASURING EXPERIMENT OF HAND MOVEMENT

The purpose of this study is to analyze human dexterity by measuring each joint angle and extracting and visualizing the characteristics involved in movements. In our study, we conducted the following two types of movement measurement experiments. The first experimental movement is a simple, repeated grasping in which the elbow is in the flexion to the extension state, and the forearm is pronation-rotated, and the fingers are flexed for grasping. The second experiment used the Purdue Pegboard Test, which evaluates finger dexterity. A human subject pinches a peg, adjusts its posture, and inserts it in a hole placed in a series. In these measurements, the two measurement systems described in Section II. A were attached to the subject (Fig. 1), and synchronous measurements were made at a sampling frequency of 100 Hz. Our experiments were conducted with one male subject in his twenties to study the differences between the identical movements by the same person. We explained our work to him, and he signed a consent form. The ethics review committee of Doshisha University approved the experiments.

A. Measurement of Simple Grasping Movement

To verify how effectively SVD assessed dexterity, we examined whether SVD and clustering can decompose a motion and extract the features contained in it. We measured a simple movement of opening a hand near the head and then grasping an object in front of the body. The results of decomposing the movements are expected to reveal their elements for adjusting the position and timing of the fingers to grasp an object and for adjusting the force during grasping. We defined the movement from the elbow's maximum bending position to the next reference point as one trial and repeatedly measured it. However, the first trial was a continuous motion from the measurement's start. To exclude the difference of the initial state in the repetitions, we extracted trials from the second trial. The measurement for 10 s including the static time for calculating initial postures 2 s, was twice.

B. Result and Discussion of Simple Grasping Movement

From the twice measurements performed by our subject, four trials were extracted. The SVD results for each trial and each mode up to the seventh mode (where the cumulative contribution was 90%) of the left and right singular value vectors were clustered. Up to the fourth mode (an average contribution of 3.9% and an average cumulative contribution of 80%), the same number of modes were clustered with distance thresholds of 1.0-1.6 (left) and 1.4-2.1 (right). The result of the left and right singular value vectors of the 1st-4th modes for one representative trial are shown in Figs. 2 and 3. Fig. 2 shows the time variation, which is the left singular value vector, and Fig. 3 shows the degree of change in the joint angles, which is the right singular value vector. The 1st mode

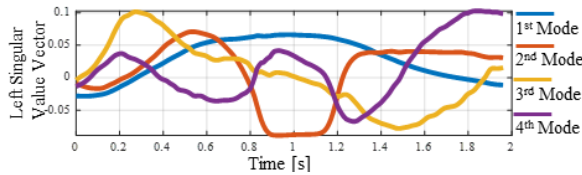


Figure 2. Time variation of left singular value vectors in simple grasping

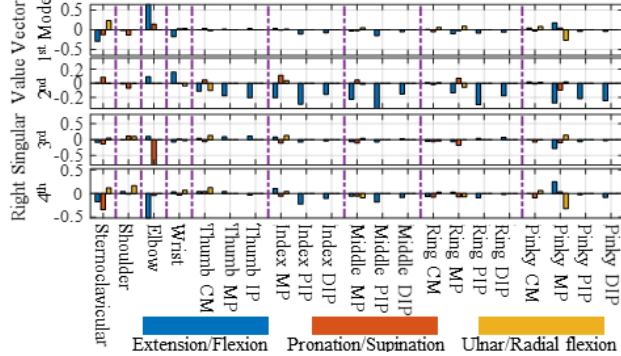


Figure 3. Joint distribution of right singular value in simple grasping

with a 47.5% contribution shows a hand movement to a grasping position by elbow extension and the sternoclavicular joint, and the hand posture is simultaneously adjusted by the forearm pronation. The 2nd mode (18.5 %) shows the fingers opened once by extension and then flexed to grasp after moving in the first mode. In addition, the posture was adjusted for easy grasping by combining elbow flexion and wrist extension. The 3rd mode shows a braking movement and adjusting by forearm supination in the opposite of the pronation direction in the first mode up to 0.6 s. The 4th mode shows an adjustment to move to the target position because the elbow flexion/extension shows a sine curve in the extension in the first half of the first mode and an inverse sine curve in the flexion in the second half of the first mode. Therefore, using this method, the main movement of the entire movement can be extracted to understand the joint coordination and timing and to evaluate the adjustment components that are expected to produce more dexterity.

C. Measurement of Pegboard Test

To evaluate the motion dexterity, the right hand (dominant) and the upper limb movement during the general Pegboard Test were measured. To measure the entire dexterity test (30 s), the measurement was performed for 40 s, including the static time. We defined one trial is process of pinching a peg, inserting it into a hole, and pinching the next peg during the entire measurement. We extracted some trials. However, for the same reason as in Section III. A and B, we excluded the first trial. Six trials from the 2nd to the 7th trial were analyzed to prevent the influence of an increase in the moving distance to the hole position and a decrease of the difference due to habituation.

D. Result and Discussion of Pegboard Test

In this experiment's analysis, we focused on the thumb and index and middle fingers because the IMU outputs on the ring and little fingers were abnormal and had no effect on the dexterity test. The trial times of the extracted 2nd-7th trials were 1.64 s, 2.15 s, 1.69 s, 1.89 s, 2.46 s, and 1.92 s. According to the dexterity test in a previous study, the average score (43 healthy subjects, 52.2 years old) was 14.7 pegs in 30 s for an average time per peg of about 2 s [4]. Therefore, in this

extraction trial, we roughly divided the trials as follows the 2nd and 4th trials into an early group, the 5th and 7th trials into an average group, and 3rd and 6th trials into a late group. Because his score was 17 pegs (1.76 s) in the pre-test without the measurement system, the 2nd and 4th trials seem less affected by the attached IMU system and show sufficient dexterity. Therefore, we analyzed the 2nd trial as the most dexterous movement.

First, Fig. 4 and 5 show the results of clustering the left and right singular value vectors up to the 7th mode, where the cumulative contribution was 90%, as in Section III. B. When we clustered them with an average distance threshold width of 1.4 (right) and 1.7 (left) from Section III. B, there were differences from the 3rd mode onward. Therefore, the cluster numbers based on the 2nd trial decomposition mode (C1, C2, ..., C7) shown in the figures were used in the following description. From the figures, the 1st and 2nd modes showed similar behavior regardless of the trial times. In the four trials with short times (the early and average groups), the combinations of joint conditions (right vector) and timing (left vector) are consistent, although the order differs up to the 6th mode, for the slow trials, the clusters of right and left vectors were different, suggesting that the movements with high contribution in a trial have appropriate time-series waveform shape and timing.

Next, to verify the timing in detail, the left singular value vectors of the 2nd (early group), the 7th (average) and the 6th (slow) trials are shown in Fig. 6 as representative trials. Because the joint relationship and the movement's purpose are also important in timing verification, the right singular value vector distribution and representative reconstructed link models (from \mathbf{A}_{ave} and each $S_m \mathbf{u}_m \mathbf{v}_m^T$ in (2)) for the 2nd trial are shown in Figs. 7, 8. In the 1st mode, the trials' main elements are performed simultaneously: moving to the target hole position (elbow flexion), the overall postural adjustment of the peg (forearm supination and wrist extension), and a light grip (each finger joint). The 2nd mode had a sine curve shape and showed that the peg posture was adjusted by three fingers at the convex part to complement the arm's postural element in the 1st mode. Based on a comparison of the three group trials, perhaps adjusting the peak of the 2nd mode aligned it to match

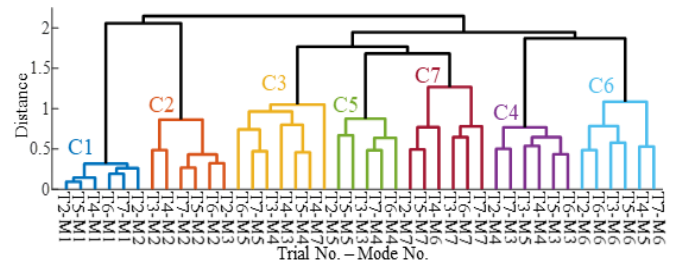


Figure 4. Clustering result of left singular value vectors in pegboard test

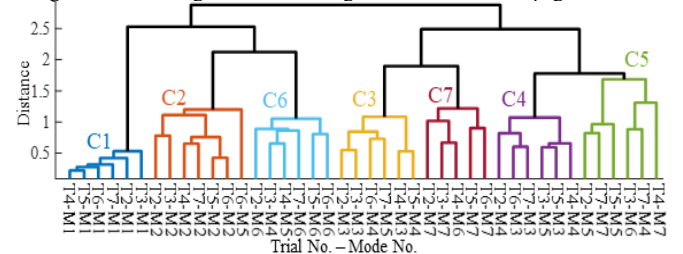


Figure 5. Clustering result of right singular value vectors in pegboard test

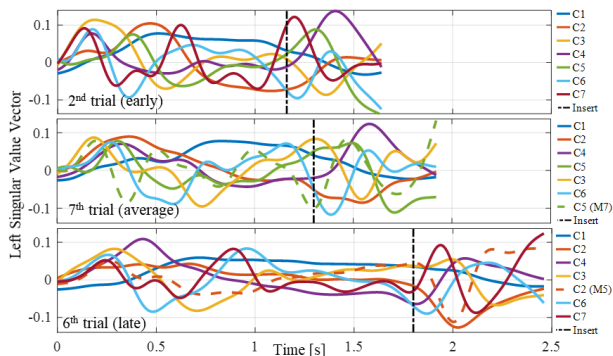


Figure 6. Time variation of left singular value vectors in pegboard test

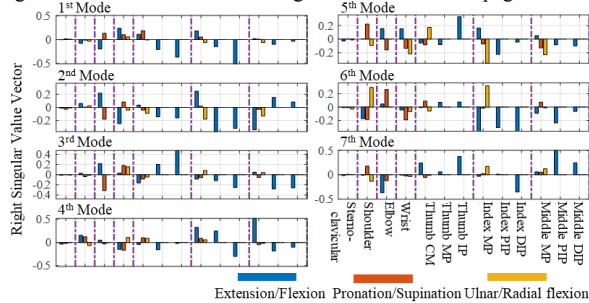


Figure 7. Joint distribution of right singular value in pegboard test

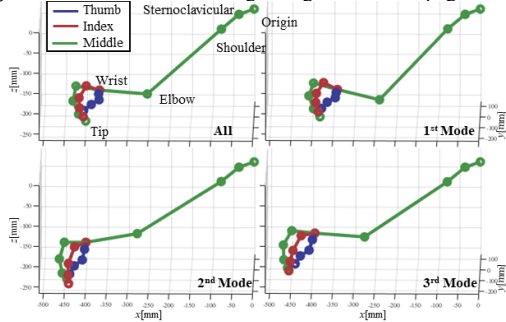


Figure 8. Measured (Left Upper) and decomposed representative mode (1st-3rd) reconstructed link models at 0.5 s in 2nd trial

the maximum arrival point of the 1st mode. Then it was considered possible to quickly adjust the peg posture by fingers to insert, by reflecting the situation of the peg posture and the hole position by the arm moving in the 1st mode. However, in the 6th trial (slow), little postural adjustment was performed by the fingers, and the lower contribution mode oscillated near the time of the peg insertion after the movement, suggesting that postural adjustment took time. C3 was pinching the peg by the fingers and the hand's downward movement, and C4 was its release by the fingers and an upward movement. As in the 3rd mode, C3 appeared in the first half trials and C4 in the second half, suggesting that the priority of the pinching and releasing movements were switched by the moved distance, although they did not significantly affect the trial time. In the remaining clusters, C5 was the moving adjustment, C6 was the pinching and releasing adjustment, and C7 was the fine postural adjustment. From the Fig. 6 and movement type, we considered that an important factor in this dexterity test was the influence of the initial timing of each mode. In 2nd and 7th trials, the initial rise of modes other than C1, C2 and C5 were rapid. In particular, focusing on the relationship between the rise timing of C3 for pinching a peg and C2 for adjusting a peg posture, the transition in the 2nd trial from C3 to C2 related to the fingers' movement was smooth because the peg posture was adjusted

after the peg was stably pinched. In contrast, in the 7th trial, the rise of C3 was the same as in the 2nd trial, but the transition to C2 started before the pinching in C3 became stable. In the 6th trial, the rise of C3 was slow, and it is highly possible that the transition to C2 was not successful because the pinching was not stable, leading to the oscillatory waveform described above. Therefore, it is important to perform C1-3, which are high contribution movements, at the appropriate timing, and it is possible to understand the movement situation in the dexterity test in addition to time indices.

Therefore, these results suggest that primary movements with large joint changes should be performed with a single synchronized timing waveform as much as possible. Dexterity movements are performed by matching the timing of low contribution with respect to such movement timings, and the transition timings between movements that are mainly homogeneous joint movements such as C2 and C3 are particularly important. Furthermore, the results suggest that if a large amount of information on each mode and the classification results from clustering can be stored and converted into a database, judgments can be made about dexterity and used for suggesting behavioral improvements based on comparison with a database when the results of the dexterity tests of new subjects are obtained.

IV. CONCLUSION

We extracted time-series joint angles from upper limb movements, including fingers that were measured in detail by IMU systems, and applied SVD and clustering to them. For the hand movement of a finger dexterity test, we identified appropriate timing and joint coordination in high dexterity trials. Unfortunately, we only collected data from a single subject. Future research must increase the number of subjects and simultaneously acquire and analyze such factors as the peg's posture and the amount of force from the fingertips.

ACKNOWLEDGMENT

This work was supported by JSPS KAKEN Grant Numbers JP21K14109 and JP19K04263.

REFERENCES

- [1] T. Abe, K. Fujii, K. Hyodo, N. Kitano, and T. Okura, "Effects of acute exercise in the sitting position on executive function evaluated by the Stroop task in healthy older adults," *The Journal of Physical Therapy Science*, Vol. 30, No. 4, (2018), pp.609-613
- [2] Y. Kimoto, T. Oku, and S. Furuya, "Neuromuscular and biomechanical functions subserving finger dexterity in musicians," *Scientific Reports* 9, 12224 (2019).
- [3] S. Aoi, et al., "Neuromusculoskeletal model that walks and runs across a speed range with a few motor control parameter changes based on the muscle synergy hypothesis," *Scientific Reports* 9, 369 (2019).
- [4] Eto F, Harasawa M, Hirai S, "Hand Dexterity Related to Age: Pegboard Test as an Indicator of Aging and Brain Dysfunction," *The Japan Geriatrics Society*, Vol. 20, No. 5 (1983), pp. 405-409, (in Japanese).
- [5] K. Kitano, A. Ito, and N. Tsujiuchi, "Hand Motion Measurement using Inertial Sensor System and Accurate Improvement by Extended Kalman Filter," *Conf. Proc. IEEE Eng Med Biol Soc.* (2019), pp. 6405-6408.
- [6] S. Jauhiainen, A. J. Pohl, S. Äyrämö, J. Kauppi, and R. Ferber, "A hierarchical cluster analysis to determine whether injured runners exhibit similar kinematic gait patterns," *Scandinavian Journal of Medicine and Science in Sports*, Vol. 30, Issue 4, 2020, pp. 732-740.